revised for *JACS,* July 25, 2017

Hyper Open-Shell States: The Lowest Excited Spin States of O Atom, Fe^{2+} Ion, and FeF_2

Zoltan Varga,[1,†] Pragya Verma,[1,2,†,*] and Donald G. Truhlar[1,2,*]

[1]*Department of Chemistry, Chemical Theory Center, and Minnesota Supercomputing Institute, 207 Pleasant Street SE, University of Minnesota, Minneapolis, MN 55455-0431*

[2]*Nanoporous Materials Genome Center, 207 Pleasant Street SE, University of Minnesota, Minneapolis, MN 55455-0431*

Abstract. Excited spin states are important for reactivity, catalysis, and magnetic applications. This work examines the relative energies of the spin states of O atom, Fe^{2+} ion, and FeF_2 and characterizes their excited spin states. Both single-reference and multi-reference methods are used to establish the character of the lowest singlet excited state of all three systems and the lowest triplet excited state of Fe^{2+} and FeF_2. We find that the conventional representation of the orbital occupancies is incorrect in that the states have more unpaired electrons than the minimum number required by their total electron spin quantum number. In particular, we find that for a given spin state, an electronic configuration with more than 2*S* unpaired electrons is more stable than the configuration with 2*S* unpaired electrons (where *S* is the spin of the system). For instance, triplet FeF_2 with four unpaired electrons is lower in energy than triplet FeF_2 with two unpaired electrons. Such highly open-shell configurations are labeled as *hyper* open-shell electronic configurations in this work and are compared to *ordinary* open-shell or closed-shell electronic configurations. The hyper open-shell states considered in this work are especially interesting because, unlike typical biradicals and polyradicals, the unpaired electrons are all on the same center. This work shows that the conventional perspective on spin-state energetics that usually assumes *ordinary* open-shells for single-centered radicals needs modification to take into account, whenever possible, *hyper* open-shell configurations as well.

1. Introduction

Molecules and solids containing transition metals are widely studied in chemistry and biology owing to the important role they play both as catalysts and intermediates in chemical reactions and their role in a variety of applications where they serve as magnetic centers.[1,2,3,4,5,6,7,8,9,10,11] Their open-shell electronic states lead to rich chemistry that arises primarily due to their ability to change oxidation state and, for a given oxidation state, to sometimes have more than one low-lying spin state. For example, more than one spin state may play a role within a single catalytic cycle, and a spin-state change from a lower spin state to a higher one or vice-versa may be required if a reaction is to proceed with a low barrier.[12,13,14] Not only can there be multiple low-energy spin states, but also there can be more than one possible electronic configuration for a given spin. Because it is imperative to ascertain the lowest-energy configuration for each spin as well as to determine the relative ordering and energy separations of the spin states, understanding the rich chemistry exhibited by open-shell compounds is not straightforward, and often the experimental results can be fully interpreted only when complemented by quantum mechanical calculations.

The widely used quantum mechanical methods for studying transition-metal-containing systems[15,16,17,18,19,20] are based on either Kohn-Sham density functional theory (KS-DFT) and wave function theory (WFT), each of which brings certain advantages to the table. A particularly interesting issue that may be addressed by both kinds of theory, but in different ways, is the question of calculating how many unpaired electrons are present in a system. A fully paired configuration has no unpaired electrons; all other systems are open-shell systems. An ordinary open-shell system has $2S$ unpaired electrons, where S is the total electronic spin (in the present article we assume that Russell-Saunders coupling provides a good description, and we neglect spin-orbit coupling, so S is a good quantum number). Configurations with more than $2S$ unpaired electrons are called hyper open-shell. Textbook depictions of open-shell systems almost always show them as ordinary open-shell systems, for example, in discussions of Hund's rules or of high-spin versus low-spin transition metal complexes.

The best-known example of a hyper open-shell system is the case of an open-shell singlet. The excited singlet state of CH_2 is a well-known example,[21,22] but is often considered to be an exceptional case. Diradicals[23,24,25,26,27,28] are another example of an open-shell singlet. The

simplest example of a diradical is a stretched single bond; for example, when ground-state singlet H_2 is stretched to a larger internuclear distance (*e.g.*, 4 Å), the correct description is that there is an unpaired electron on each center. There are several other examples in the literature of molecules that have been described to have unusual electronic configurations,[29] including a doublet with three unpaired electrons,[30] and these configurations become especially important when they play a role in reactivity.[31,32,33] Although diradicals and even polyradicals are well known in chain molecules,[34,35,36] which can have radical sites spaced along a chain, the importance of hyper open-shell systems with all the unpaired electrons on the same atom seems to be less widely appreciated (and is certainly less commonly discussed). We call such systems intra-atomic hyper open-shell systems.

The main objective of the present article is to emphasize the occurrence of intra-atomic hyper open-shell configurations and compare their energies to those of ordinary open-shell configurations. We will illustrate our discussion by considering ^{1}D oxygen atom and the lowest-energy singlet and triplet states of Fe^{2+} ion and the FeF_2 molecule, where the latter can be viewed as a prototype of an iron complex. We not only find that these species are intra-atomic hyper open-shell cases, but we also find that there can be a greater degree of open-shell character than the minimum required for hyper open-shell species; in particular, we find singlets with four unpaired electrons. We believe that intra-atomic hyper open-shell states are not unique to the O atom, Fe^{2+} ion, or FeF_2 molecule, and the analysis presented here has broad implications for compounds that have open-shell configurations. This changes the conventional perspective on spin-state energetics.

The wave function of many open-shell systems cannot be described well by a single Slater determinant or a single configuration state function (CSF), where a CSF is defined as a linear combination of Slater determinants with the combination coefficients chosen to give it the correct spin symmetry and a convenient spatial symmetry. Systems that are not well described by a single Slater determinant or a single CSF are variously called inherently multi-configurational systems or strongly correlated systems (from a physics point of view) or multi-reference systems (from a method point of view). High-accuracy wave function methods usually have two steps: first, the calculation of a reference function, and second, adding dynamic correlation or more dynamic correlation to it. For the most accurate results, the treatment of multi-reference systems usually requires either a multi-configurational reference function or very high-order excitations

(*e.g.*, quadruple excitations or higher) from a single Slater determinant or single CSF. Note that some types of multi-configurational wave functions can be described or approximated by a single-reference formalism, *e.g.*, the spin-flip method.[37] The present study employs multiconfigurational WFT calculations to obtain best estimates of excitation energies and the effective number of unpaired electrons. The quantification of this concept is not trivial, and there exist a number of approaches.[38,39,40,41,42,43] We use indices proposed by Takatsuka, Fueno, Yamaguchi, Staroverov, Davidson, and Head-Gordon.[38,39,42] We compare wave functions computed by different approaches to compare effective numbers of unpaired electrons calculated from WFT calculations designed to include static correlation, WFT calculations designed to include static and dynamic correlation, and DFT calculations, where in the DFT case we determine the number of unpaired electrons based on orbital diagrams.

This paper is organized as follows. Section 2 discusses the DFT and WFT methods used in this work, Sections 3 presents the O atom, Fe^{2+} ion, and FeF_2 molecule examples, respectively, and Section 4 has concluding remarks.

2. Methods

A combination of DFT and WFT is used to understand the electronic configurations of various spin states of O atom, Fe^{2+} ion, and FeF_2 molecule and to predict spin-state energies of these species.

DFT calculations. Among the three species investigated, only FeF_2 is a molecule, and its geometry in the quintet spin state is known from experiments,[44] but the geometries of the triplet and singlet spin states are not known. Therefore we optimized the geometries of all the three spin states using DFT. The DFT method used for optimization is the combination of the M06-L[45] exchange-correlation functional with the def2-TZVP (TZVP = "triple-zeta-valence polarized")[46] basis set. This method is chosen because it gives an accurate prediction for the geometry of the experimentally[44] known quintet state. The “UltraFine” grid that has 99 radial shells and 590 angular points for every radial shell was used for all the calculations. The geometry optimizations involved finding the minimum-energy structures and confirming that they are minima by doing harmonic vibrational frequency calculations.

Except when explicitly mentioned that we are calculating an unstable state, all SCF calculations were performed by doing stability checks in *Gaussian 09*,[47] and when the Slater determinant was unstable,[48,49,50] breaking of symmetry was allowed to find a stable solution of the SCF equations, with the only constraint being the value of the total electronic spin component M_S, which is set to $M_S = S$ for the target spin state with total electron spin S. As a result of symmetry breaking, the *p* and *d* orbitals of atoms no longer constitute degenerate subshells; this is not an error – it is the way that Kohn-Sham DFT represents the density of multiconfigurational wave functions by the density of a Slater determinant.[51] Some discussion of the orbital pictures provided by broken-symmetry Kohn-Sham solutions for transition metal complexes has been provided in a previous article.[52]

The optimized structures of the quintet, triplet, and singlet were used for single-point calculations with DFT and WFT. For DFT, the relative energies of various spin states of O atom, Fe^{2+} ion, and FeF_2 molecule were determined from single-point calculations with the cc-pwCV5Z-DK[53,54,55] basis set and the M06[56] exchange-correlation functional in *Gaussian*. The cc-pwCV5Z-DK basis set includes core-valence correlation and is optimized for scalar relativistic calculations; it was used with the second-order Douglas-Kroll-Hess scalar relativistic Hamiltonian.[57,58,59,60] In the M06 calculations, the "UltraFine" grid was used and calculations were performed both with and without the stability check option. The WFT calculations are explained in the next subsection.

To explain the spin purification scheme used here we introduce the notation that E_M is the energy of the optimized Slater determinant with spin component M_S equal to M, where M is 2, 1, or 0, and $\langle S^2 \rangle_M$ is the expectation value of S^2 in the calculation with M_S equal to M. In the DFT calculations, some of the Slater determinants have $\langle S^2 \rangle_M$ not equal to $M(M + 1)$ as would be the case for a spin eigenfunction. For O atom two spin states (singlet and triplet) were calculated, and for Fe^{2+} ion and FeF_2 three spin states (quintet, triplet, and singlet) were calculated. The singlet state of O atom has spin contamination from the triplet state, and those of Fe^{2+} ion and FeF_2 have spin contamination from both the triplet and quintet states. The triplet states of Fe^{2+} ion and FeF_2 have contamination from the quintet state. Because the conventional Yamaguchi spin-purification scheme,[61,62,63,64,65] does not lead to reasonable values when used for multiplicities higher than singlet and triplet, we use the weighted-average broken-symmetry

(WABS) method given by equations 1 and 2,[66] where a broken-symmetry solution in this context is indicated by an $\langle S^2 \rangle$ value greater than $M(M + 1)$.

$$E_{M-1}^{\mathrm{WABS}} = E_M - k\left(E_M - E_{M-1}\right) \tag{1}$$

where

$$k = 2S_M \Big/ \left(\left\langle S_M^2 \right\rangle - \left\langle S_{M-1}^2 \right\rangle\right) \tag{2}$$

The WABS method has been successfully used in our earlier work for 3*d* transition metals and their ions[19] and by other workers as well.[67]

For Fe^{2+} and FeF_2 spin contamination is removed from the triplet state by using the quintet state as the high-spin state, and for O atom it is removed from the singlet state by using the triplet state as the high-spin state. The spin contamination from the singlet state of Fe^{2+} ion and FeF_2 was not removed because it is ambiguous how to conveniently remove spin contamination when it comes from two higher-spin states, namely the triplet and quintet. In any event, "removal" of spin contamination, although it usually improves the accuracy, is not guaranteed to do so,[19] and our main conclusions do not rely on it.

Single-point WFT calculations. The relative energies of various spin states of O, Fe^{2+}, and FeF_2 were determined from single-point calculations using WFT with the cc-pwCV5Z-DK basis set, the second-order Douglas-Kroll-Hess scalar relativistic Hamiltonian, and the *Molpro*[68,69] computer program.

In the WFT calculations, D_{2h} symmetry was applied for all three systems. Complete active space self-consistent field (CASSCF)[70,71,72] calculations on the oxygen atom were done using the (6e, 4o) active space that has six electrons in 2*s* and 2*p* orbitals, and CASSCF calculations on Fe^{2+} ion and FeF_2 were done using the (6e, 5o) active space that has six electrons in five 3*d* orbitals. The CASSCF calculations were done in two ways, *i.e.*, both as state-averaged (SA) and state-specific (SS) calculations. To add more dynamic correlation energy and get accurate energies, the multi-reference averaged coupled-pair functional (MR-ACPF)[73,74] method was used with SS-CASSCF reference wave functions in which single-state calculations for each spin state were carried out only for the first states in each irreducible representation. Multi-reference configuration interaction (MRCI) calculations[75,76,77] were also carried out for all states based on the SA-CASSCF reference wave functions. Both the valence and outermost core electrons were included in dynamic electron correlation, which is denoted by FC−1.

The CASSCF and MRCI wave functions were used to calculate the effective number of unpaired electrons in each state. There is more than one formalism for analyzing this,[38,39,40,41,42,43,78,79,80,81] and we used three of them. In general, the number of unpaired electrons can be expressed as

$$n_X = \mathrm{tr}(\mathbf{V} f_X(\mathbf{n}) \mathbf{V}^\dagger) \quad (3)$$

where tr denotes a trace, **V** is the natural orbital basis, **n** is the diagonal matrix of eigenvalues of the density matrix, and the diagonal elements of $f_X(\mathbf{n})$ can be expressed in different ways, denoted by U or S or D. Here U referes to Head-Gordon's U index given by eq 4:[39]

$$[f_U(\mathbf{n})]_i = 1 - |1 - n_i|, \quad (4)$$

S referes to Head-Gordon's S index given by eq 5:[39]

$$[f_S(\mathbf{n})]_i = n_i^2 (2 - n_i)^2, \quad (5)$$

and D refers to the index of Takatsuka, Fueno, and Yamaguchi[38] given by eq 6:

$$[f_D(\mathbf{n})]_i = 2n_i - n_i^2 \quad (6)$$

where n_i is the natural orbital occupation number (NOON) of natural orbital i for a given single state (rather than the average). Note that the index of Takatsuka, Fueno, and Yamaguchi is the same as the one proposed by Staroverov and Davidson.[42]

In CASSCF calculations the total number of electrons in the active space is well defined, and it is enough if calculations of the effective number of unpaired electrons use only the occupation numbers of the orbitals in the active space. The occupation number of inactive orbitals is two and that of virtual orbitals is zero; therefore their contribution to the effective number of unpaired electrons is inherently zero. But for MRCI, there are many morre orbitals with nonzero NOON. We calculated the NOON values of the active space orbitals in the MRCI calculations, and these numbers are only slightly different (by less than 0.04 electrons) from the CASSCF occupation numbers. Based on occupation number agreement between the two methods, the NOON values of the active space orbitals are used to approximate the effective numbers of unpaired electrons from MRCI calculations as well.

Experimental data. To compare calculated values with the experimental relative energies of the spin states of O atom and Fe^{2+} ion,[82] we calculated the spin-free energies[19,20] from the experimental data. The spin-free energies are the ones from which spin-orbit coupling has been removed, and they are obtained from the experimental data by taking the $(2J + 1)$-weighted

average over the components of the mutliplet, where *J* is the total angular momentum quantum number.

Excitation energies. We define the relative energy of a spin state as the difference between the energy of the lowest state with a given *S* and the energy of the ground state (with the ground-state value of *S*).

3. Results and Discussion

3.1. Oxygen atom

In this section we consider triplet and singlet spin states of O atom. We will use this simple case to discuss some of the complications in analyzing open-shell states, and we will show how both single-reference DFT calculations and multiconfigurational WFT calculations lead to the conclusion that the ^{1}D state of O is an open-shell singlet. We note that this conclusion about the lowest excited state of the oxygen atom is contrary to the generally accepted[83] view, which considers it to be a closed-shell singlet. Using the nomenclature defined above, the open-shell singlet is an intra-atomic hyper open-shell (HOS) singlet.

Excitation energy of singlet O. For O atom, the excitation energy (defined at the end of section 2) is the difference in excitation energy of the first excited state, which is a singlet, from the ground state, which is a triplet.

Tables 1 and 2 present the excitation energy of singlet O atom calculated by M06 and MR-ACPF, respectively. Both the methods correctly show that the triplet state is the ground spin state (^{3}P), and that the first excited state is a singlet (^{1}D). The first excitation energy calculated from MR-ACPF (45.4 kcal/mol) agrees very well with the experimental excitation energy of 45.1 kcal/mol, while the excitation energy from M06 deviates significantly. This gets greatly improved with the spin purification scheme of eq 1 that removes spin contamination from the singlet state and leads to a deviation of only ~2 kcal/mol from experiments. The usefulness of the M06 exchange-correlation functional for such systems along with spin-projection schemes for accurately predicting singlet–triplet energy gaps with DFT is also shown in Table 3 of Ref. 84. Another formulation of spin purification scheme, which yields a result very similar (47.3 kcal/mol) to that given in Table 1, is reported in Supporting Information.

Table 1. Relative energies (ΔE in kcal/mol)[a] of O atom with and without spin-projection and $\langle S^2 \rangle$ values calculated using M06/cc-pwCV5Z-DK.

State	Type[b]	ΔE_{M06}	$\langle S^2 \rangle$	$\Delta E_{expt.}$[c]
^{3}P	OOS	0.0	2.01	0.0
^{1}D	HOS	23.7,[d] 47.1[e]	1.00[d]	45.1
–	CS	61.2[f]	0.00[f]	–

[a] ΔE is calculated with respect to the triplet spin state.

[b] OOS = ordinary open-shell, HOS = hyper open-shell, CS = closed-shell

[c] spin-free values derived from Ref. 82

[d] directly calculated variational result

[e] obtained by the weighted-average broken-symmetry (WABS) spin-projection method of eq 1

[f] unstable solution

Orbital energy diagram. To illustrate the energetic lowering of the HOS state as compared to the lowest-energy closed-shell (CS) singlet, we also performed a DFT calculation of the unstable lowest-energy closed-shell singlet. Table 1 shows that the CS restriction raises the energy by 14 kcal/mol, and Figure 1 is an orbital energy diagram that helps us to understand why the HOS state is lower in energy than the closed-shell singlet. This figure shows that the ground state of oxygen atom is an ordinary open-shell (OOS) state, in particular an ordinary triplet with two unpaired electrons (both α spin), and the first excited state singlet state also has two unpaired electrons (although now there is one α and one β), so it is not an ordinary singlet, but rather is an HOS state. We also show the orbital energies for the lowest-energy CS singlet solution of the SCF equations. We see that the two singly occupied orbitals in the ^{1}D state have the same energy due to spatial degeneracy of the 2*p* orbitals, and the average *p* orbital energy is lower than in the CS state. The $\langle S^2 \rangle$ value for the HOS state shows high spin contamination, and a large correction for energy (more than 20 kcal/mol) is obtained by spin purification (see Table 1). Although the spin purification scheme allows one to conveniently remove spin contamination from the energy, it does not change the nature of the Slater determinant, which remains spin contaminated. Hence one might question whether the greater number of unpaired electrons as compared to the CS state is an artifact of mixing in the unpaired-electron character of lower energy triplet. That motivated us to analyze wave functions of the various states of oxygen atom using WFT with pure spin states, as described next.

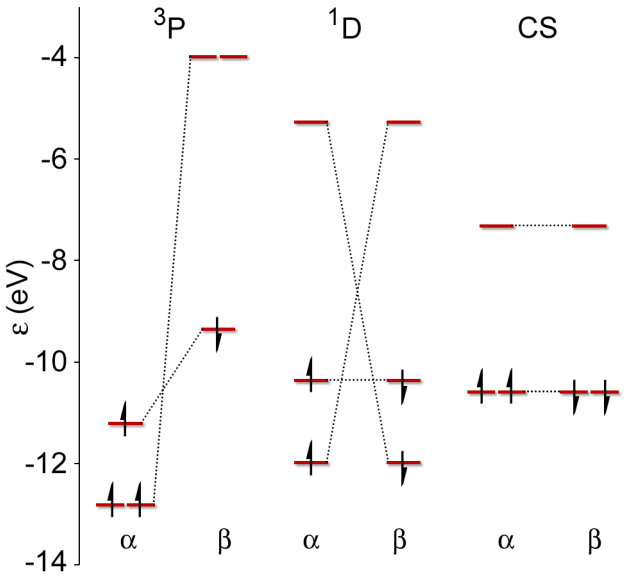

Figure 1. Orbital energy diagrams of the 2*p* orbitals of the three states (^{3}P, ^{1}D, and CS) of O atom from M06/cc-pwCV5Z-DK calculations. The dotted lines connect an orbital in the α manifold to the corresponding orbital in the β manifold.

We need to consider spatial degeneracy, but since spin-orbit coupling is not included in this article, we do not need to consider spin degeneracy in discussing the quantum mechanical calculations. In the WFT calculations we find that the ground spin state of O atom has three-fold spatial degeneracy (P character) and the first excited state has five-fold spatial degeneracy (D character) as shown in Table 2. We applied D_{2h} symmetry in the calculations, and the 2*s*, $2p_x$, $2p_y$, and $2p_z$ orbitals belong to a_g, b_{3u}, b_{2u}, and b_{1u} irreducible representations, respectively, from which the CSFs are constructed. One way to analyze the wave function of both the triplet and singlet states is to look at the individual CSFs and their occupation numbers. First let's consider the triplet ground state – the 2*s* orbital is doubly occupied, one of the 2*p* orbitals is also doubly occupied, and the other two 2*p* orbitals are singly occupied, where both the electrons have same spin. It has three possible solutions where any of the $2p_x$, $2p_y$, and $2p_z$ can be the doubly occupied one. The symmetries for the wave functions arising from these three possibilities are given below, where each wave function represents a CSF with equal energies (as shown in Table 2):

$$- (a_g)\times(a_g)\times(b_{3u})\times(b_{3u})\times(b_{2u})\times(b_{1u}) = B_{3g}$$

$$- (a_g)\times(a_g)\times(b_{2u})\times(b_{2u})\times(b_{3u})\times(b_{1u}) = B_{2g}$$

$$- (a_g)\times(a_g)\times(b_{1u})\times(b_{1u})\times(b_{2u})\times(b_{3u}) = B_{1g}$$

Table 2. Relative energies (ΔE in kcal/mol) and effective numbers of unpaired electrons of O atom calculated using SA-CASSCF/cc-pwCV5Z-DK, MRCI/cc-pwCV5Z-DK, and MR-ACPF/cc-pwCV5Z-DK.[a]

State	Type[b]	Irrep[c]	$\Delta E_{\text{SA-CASSCF}}$	$\text{ENUE}_{\text{CASSCF}}$			$\text{ENUE}_{\text{MRCI}}$			$\Delta E_{\text{MR-ACPF}}$	$\Delta E_{\text{expt.}}$[e]
				n_U	n_S	n_D	n_U	n_S	n_D		
^{3}P	OOS	B_{1g}	0.0	2.00	2.00	2.00	2.04	2.00	2.10	0.0	0.0
	OOS	B_{2g}	0.0	2.00	2.00	2.00	2.04	2.00	2.10	0.0	0.0
	OOS	B_{3g}	0.0	2.00	2.00	2.00	2.04	2.00	2.10	0.0	0.0
^{1}D	HOS	A_g	50.3	1.72	1.88	2.00	2.03	2.00	2.09	45.4	45.1
	HOS	A_g	50.3	1.38	1.52	2.00	1.38	1.45	2.08	[d]	45.1
	HOS	B_{1g}	50.3	2.00	2.00	2.00	2.03	2.00	2.09	45.4	45.1
	HOS	B_{2g}	50.3	2.00	2.00	2.00	2.03	2.00	2.09	45.4	45.1
	HOS	B_{3g}	50.3	2.00	2.00	2.00	2.03	2.00	2.09	45.4	45.1

[a] ΔE is calculated with respect to the ground state triplet. ENUE denotes effective number of unpaired electrons.

[b] OOS = ordinary open-shell, HOS = hyper open-shell

[c] Irrep = irreducible representation

[d] MR-ACPF can be calculated only for the first state in each irrep.

[e] Spin-free values derived from Ref. 82

Next if we consider the five-fold degenerate first excited state (^{1}D) of oxygen atom, we see that these five states have the following symmetries of wave functions among the irreducible representations of D_{2h}: two of A_g symmetry and one each of B_{1g}, B_{2g}, and B_{3g} symmetry. The three states with symmetries B_{1g}, B_{2g}, and B_{3g} cannot be closed-shell solutions, because if they were closed-shell solutions, then the direct product of α and β electrons in the same orbital would lead to an a_g character, and the symmetry of such a wave function has to be A_g. Therefore assuming the three states with symmetries B_{1g}, B_{2g}, and B_{3g} to be open-shell solutions with two unpaired electrons (one with α and one with β spin) will give us three possible wave functions, which are follows:

$$- (a_g)\times(a_g)\times(b_{3u})\times(b_{3u})\times(b_{2u})\times(b_{1u}) = B_{3g}$$

$$- (a_g)\times(a_g)\times(b_{2u})\times(b_{2u})\times(b_{3u})\times(b_{1u}) = B_{2g}$$

$$- (a_g)\times(a_g)\times(b_{1u})\times(b_{1u})\times(b_{2u})\times(b_{3u}) = B_{1g}$$

Here a pair of CSFs represents each wave function, where the only difference between the pair is the switching of the α and β electrons. The rest of the two states of the five-fold degenerate ^{1}D

state belong to A_g symmetry, as mentioned above. It was also mentioned that all of the closed-shell solutions have to belong to this symmetry, and open-shell solutions can also have this symmetry if the direct product of the irreps of unpaired electrons is A_g. But it is impossible for only two electrons to give this symmetry if they do not belong to the same irrep. In the A_g symmetry the wave function has to be described by linear combinations of closed-shell CSFs. There are altogether four possible CSFs – one of the 2*s* or 2*p* orbitals is empty and the other three orbitals are doubly occupied. Of these four CSFs, three CSFs (where 2*s* orbital is doubly occupied) are used to describe the two A_g states of the five-fold degenerate ^{1}D state. We are not surprised that an open-shell singlet can be constructed entirely from closed-shell CSFs because we have a familiar example, namely that of the stretched-H_2 open-shell singlet (which was mentioned in the introduction); it can be described by a linear combination of σ_g^2 and σ_u^2.

Effective number of unpaired electrons. We used the recipes given in Section 2 to compute the effective number of unpaired electrons in each component state of the SA-CASSCF and MRCI wave functions for triplet and singlet oxygen atom. The effective number of unpaired electrons was computed for the components of ground state and the components of the first excited state and is tabulated in Table 2. As can be seen from the table, the effective number of unpaired electrons corresponding to the more accurate MRCI wave function lies between 1.4 and 2.1 for these states and indicates that they have about two unpaired electrons. This shows that the ^{1}D state of O atom is not a closed-shell state, and it can be described as intra-atomic HOS singlet as shown in Figure 1. The effective numbers of unpaired electrons confirm what we surmised from DFT.

The oxygen ^{1}D state is fivefold degenerate, and therefore there is considerable freedom in how to choose the eigenfunctions. One can write closed-shell functions, such as the complex ones with $M_L = \pm 2$, and one can write open-shell functions such as the complex ones with $M_L = \pm 1$. One can take linear combinations of closed-shell configuration state functions that yield open-shell ones and vice versa.[28] But any set of five orthogonal functions should have the same ensemble average for the natural orbital occupancies. It is interesting that we find an ensemble average of 4/3. Without considering the configuration state functions this could have been anticipated on the basis of symmetry (the ensemble average must be spherically symmetric). The number of unpaired electrons is not invariant to transformations among the orbitals, and even for a given choice of orbitals, it is not a physical observable[42] and therefore different definitions of

this quantity do not agree. But the point of considering the configuration state functions is that we see that the ensemble average does not involve five closed-shell wave functions. Thus the ^{1}D state should not be considered a closed-shell singlet. It is a mixed open-shell–closed-shell singlet, and therefore it has some open-shell character. The oxygen atom is actually more complicated than the cases one usually confronts in practice where either there are no degenerate orbitals or a twofold degenerate orbital of *e* symmetry. And in fact our discussion of FeF_2 below does not suffer from these complexities. But it is useful to consider oxygen because it is a simple case that is often misinterpreted as a straightforward closed-shell singlet, and it is interesting to see what happens when methods designed for lower-symmetry are applied to this textbook high-symmetry case.

3.2. Fe^{2+} ion

In this section we consider three spin states (quintet, triplet, and singlet) of Fe^{2+} monatomic ion. The ^{5}D quintet ground state of Fe^{2+} has fivefold spatial degeneracy and is an ordinary open-shell state with four unpaired electrons. Experimentally, the first excited state is the ^{3}P state with threefold spatial degeneracy, and and the second excited state is a ^{3}H state with 11-fold spatial degeneracy. The spin-free energy difference between these excited states is only 0.6 kcal/mol, and this very small energy difference is not properly treated in the calculations. In fact, even very high-level calculations may give the wrong energy order for these two triplet excited states. Therefore in the multiconfigurational calculations both states are considered. The first singlet state is a ^{1}I state with 13-fold spatial degeneracy. We will show using both DFT and WFT that the lowest-energy triplet and singlet states are hyper open-shell states.

Relative energies of spin states. Tables 3 and 4 give the relative energies of spin states of Fe^{2+} ion as calculated by M06 and MR-ACPF, respectively. Both methods agree with experiment that the quintet state is the ground spin state and that the next two higher-energy states, in order of increasing energy, are triplet and singlet; we note that this result was also obtained in our previous study[52] on relative energies of spin states of Fe^{2+} ion. The energies of the triplet and singlet states from MR-ACPF match very well with the experimental values, while M06 underestimates the excitation energies of both excited spin states by ~10 kcal/mol (if we

compare experiments to the HOS values). One possible source of this underestimate is spin contamination by the lower-energy higher-spin states. To eliminate spin contamination, we use the WABS method for the quintet-triplet pair (see eqs 1 and 2) that removes spin contamination from the HOS triplet state and gives a relative energy of 61.8 kcal/mol, which is closer to experimental (^{3}P) value of 56.1 kcal/mol than the uncontaminated case with 46.4 kcal/mol relative energy. Also shown in Table 3 are the energies of unstable excited triplet (OOS) and singlet (CS) SCF solutions that are pure spin states with no spin contamination. They are respectively 42 and 59 kcal/mol higher in energy than the corresponding ground triplet and singlet states (HOS states), and these energy differences can be attributed to the difference in electronic configurations, which is analyzed in detail next.

Table 3. Relative energies (ΔE in kcal/mol)[a] with and without spin-projection and $\langle S^2 \rangle$ values of Fe^{2+} ion calculated using M06/cc-pwCV5Z-DK.

State	Type[b]	ΔE_{M06}	$\langle S^2 \rangle$	$\Delta E_{expt.}$[c]
quintet	OOS	0.0	6.01	0.0
triplet	HOS	46.4,[d] 61.8[e]	3.00[d]	56.1
	OOS	103.9[f]	2.00[f]	
singlet	HOS	71.2	1.90	85.6
	CS	130.0[f]	0.00[f]	

[a] ΔE is calculated with respect to the quintet spin state.
[b] OOS = ordinary open-shell, HOS = hyper open-shell, CS = closed-shell
[c] Spin-free values derived from Ref. 82, where quintet is ^{5}D, triplet is ^{3}P, and singlet is ^{1}I
[d] variational solution
[e] obtained by the weighted-average broken-symmetry (WABS) spin-projection method of eq 1
[f] unstable solution

Orbital energy diagram. Figure 2 compares the M06 orbital energies of the three spin states of Fe^{2+} to one another and to those from unstable restricted SCF solutions; only the valence 3*d* orbitals are plotted. The diagram for the quintet state is straightforward, and it corresponds to an ordinary open-shell state with four α unpaired electrons, while the triplet and singlet states can have more than one way of occupying electrons in the valence 3*d* subshells. The triplet is shown with two ways of occupying orbitals – the OOS triplet solution that has two α unpaired electrons and the HOS triplet state that has three α and one β unpaired electrons. Similarly the singlet has two very different configurations in the plot, the CS singlet solution that has no

unpaired electrons and the HOS singlet state that has two α and two β unpaired electrons. There can possibly be more ways to occupy the orbitals than the ones presented here, but the ones presented are the lowest-energy ones that we were able to generate for each type.

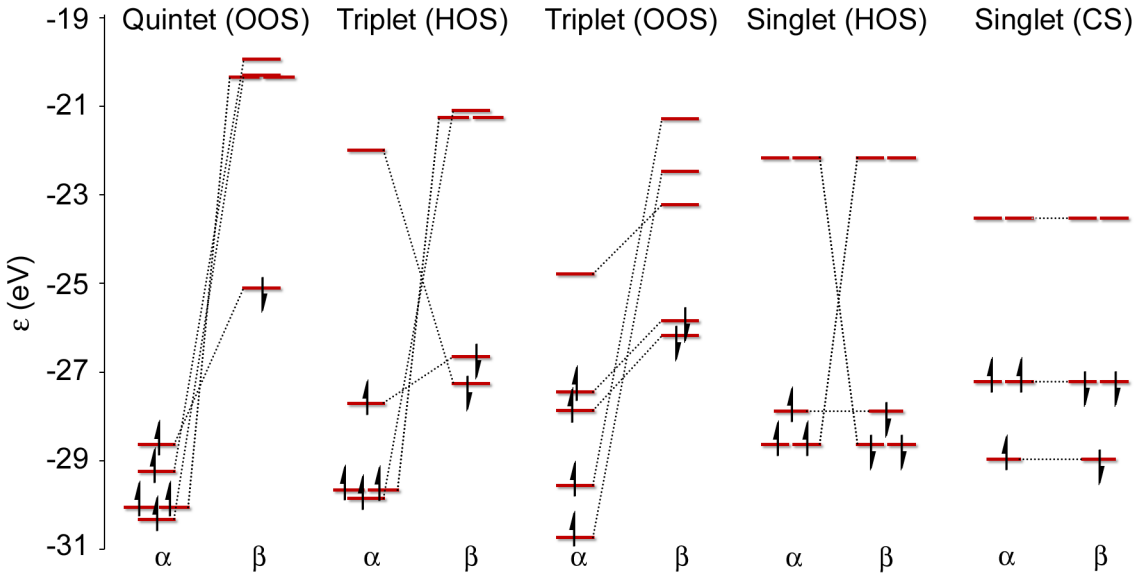

Figure 2. Orbital energy diagrams of the 3*d* orbitals of the five states (OOS quintet, HOS and OOS triplet, and HOS and CS singlet) of Fe^{2+} ion from M06/cc-pwCV5Z-DK calculations. The dotted lines connect an orbital in the α manifold to the corresponding orbital in the β manifold. [OOS = ordinary open-shell, HOS = hyper open-shell, and CS = closed-shell]

Effective number of unpaired electrons. The number of CSFs for Fe^{2+} ion is very high, and each wave function of the triplet and singlet states is a linear combination with significant contributions from many CSFs; nevertheless the effective number of unpaired electrons provides a measure of the number of unpaired electrons. Similarly to our treatment of O atom, we use the SA-CASSCF and MRCI wave functions to calculate the effective number of unpaired electrons for Fe^{2+} ion. The five components of the quintet state each have 4.0 unpaired electrons (see Table 4) by all methods, and thus the ground state is an OOS. The three spatial componets of the triplet state have effective numbers of unpaired electrons in the range of 3.59–4.59, so the triplet is an HOS and can be described as intra-atomic HOS based on Figure 2 (the effective number of unpaired electrons for an OOS would be 2.00). The singlet state hs 13-fold spatial degeneracy and its componets have effective numbers of unpaired electrons in the range 3.28–4.56, so it too is an intra-atomic HOS. Note that the effective numbers of unpaired electrons calculated using

the n_D approach are higher than those for the other two approaches (n_U and n_S), which is the expected result as discussed in ref. 78.

Table 4. Relative energies (ΔE in kcal/mol) and effective numbers of unpaired electrons of Fe^{2+} calculated using SA-CASSCF/cc-pwCV5Z-DK, MRCI/cc-pwCV5Z-DK, and MR-ACPF/cc-pwCV5Z-DK.[a]

State	Type[b]	Irrep[c]	$\Delta E_{\text{SA-CASSCF}}$	$\text{ENUE}_{\text{CASSCF}}$			$\text{ENUE}_{\text{MRCI}}$			$\Delta E_{\text{MR-ACPF}}$	$\Delta E_{\text{expt.}}$[e]
				n_U	n_S	n_D	n_U	n_S	n_D		
^{5}D	OOS	A_g	0.0	4.00	4.00	4.00	4.00	4.00	4.04	0.0	0.0
	OOS	A_g	0.0	4.00	4.00	4.00	4.00	4.00	4.04	[d]	0.0
	OOS	B_{1g}	0.0	4.00	4.00	4.00	4.00	4.00	4.04	0.0	0.0
	OOS	B_{2g}	0.0	4.00	4.00	4.00	4.00	4.00	4.04	0.0	0.0
	OOS	B_{3g}	0.0	4.00	4.00	4.00	4.00	4.00	4.04	0.0	0.0
^{3}P	HOS	B_{1g}	71.2	4.00	4.60	4.80	4.03	4.63	4.81	[d]	56.1
	HOS	B_{2g}	71.2	4.00	4.60	4.80	4.03	4.63	4.81	[d]	56.1
	HOS	B_{3g}	71.2	4.00	4.60	4.80	4.03	4.63	4.81	[d]	56.1
^{3}H	HOS	A_g	64.0	4.00	4.25	4.56	4.02	4.28	4.58	57.6	56.7
	HOS	A_g	64.0	3.87	4.25	4.56	3.90	4.28	4.58	[d]	56.7
	HOS	B_{1g}	64.0	4.00	4.24	4.56	4.04	4.27	4.58	57.5	56.7
	HOS	B_{1g}	64.0	3.87	4.25	4.56	3.90	4.28	4.58	[d]	56.7
	HOS	B_{1g}	64.0	3.59	4.14	4.54	3.62	4.18	4.56	[d]	56.7
	HOS	B_{2g}	64.0	3.75	4.17	4.53	3.78	4.20	4.55	57.5	56.7
	HOS	B_{2g}	64.0	3.82	4.23	4.57	3.83	4.26	4.59	[d]	56.7
	HOS	B_{2g}	64.0	3.74	4.16	4.52	3.77	4.19	4.54	[d]	56.7
	HOS	B_{3g}	64.0	3.75	4.17	4.53	3.78	4.20	4.55	57.5	56.7
	HOS	B_{3g}	64.0	3.82	4.23	4.56	3.84	4.26	4.59	[d]	56.7
	HOS	B_{3g}	64.0	3.74	4.16	4.52	3.77	4.19	4.54	[d]	56.7
^{1}I	HOS	A_g	95.8	3.97	4.01	4.12	4.00	4.02	4.15	86.4	85.6
	HOS	A_g	95.8	3.52	3.88	4.31	3.61	3.93	4.27	[d]	85.6
	HOS	A_g	95.8	3.70	4.01	4.32	3.75	4.00	4.27	[d]	85.6
	HOS	A_g	95.8	3.28	3.76	4.31	3.30	3.80	4.34	[d]	85.6
	HOS	B_{1g}	95.8	3.95	4.00	4.01	3.97	4.00	4.05	86.4	85.6
	HOS	B_{1g}	95.8	3.88	4.13	4.42	3.90	4.16	4.44	[d]	85.6
	HOS	B_{1g}	95.8	3.46	3.82	4.32	3.49	3.85	4.34	[d]	85.6
	HOS	B_{2g}	95.8	3.85	4.10	4.43	3.90	4.13	4.47	86.5	85.6
	HOS	B_{2g}	95.8	3.58	3.77	4.17	3.62	3.80	4.28	[d]	85.6
	HOS	B_{2g}	95.8	3.68	4.18	4.54	3.77	4.22	4.56	[d]	85.6
	HOS	B_{3g}	95.8	3.85	4.09	4.43	3.89	4.13	4.46	86.5	85.6
	HOS	B_{3g}	95.8	3.58	3.76	4.17	3.62	3.80	4.28	[d]	85.6
	HOS	B_{3g}	95.8	3.69	4.18	4.53	3.77	4.21	4.55	[d]	85.6

[a] ΔE is calculated with respect to the quintet spin state. ENUE denotes effective number of unpaired electrons.

[b] OOS = ordinary open-shell, HOS = hyper open-shell

[c] Irrep = irreducible representation

[d] MR-ACPF can be calculated only for the first state in each irrep.

[e] Spin-free values derived from Ref. 82

3.3. FeF_2 molecule

The FeF_2 molecule is linear ($D_{\infty h}$) in all three spin states with calculated bond lengths of 1.754 Å (quintet), 1.735 Å (triplet), and 1.741 Å (singlet). The many-fold degenerate spin states of Fe^{2+} ion split with the introduction of two F^- ligands in FeF_2. For instance, the five-fold degenerate quintet state splits into two Δ states, two Π states, and one Σ state. These quintet states have different energies based on which 3*d* orbital is doubly occupied. The relative energies of triplet and singlet states are even more complicated as each of these spin states can have different energies not just because of which 3*d* orbital(s) is doubly occupied, but also because of the fact that they can have OOS or HOS character, as was shown for the case of Fe^{2+} ion. In our previous two examples, an atom and an ion were used to demonstrate the difference between an OOS and an HOS, but here we use a molecule as an example and show using both DFT and WFT that there can be significant difference between both of them.

Relative energies of spin states. In contrast to the O atom and the Fe^{2+} ion, experimental spin-state relative energies are not available for FeF_2. We use the MR-ACPF values as our reference for FeF_2 as it gave good agreement with experiments for O atom and Fe^{2+} ion (see Tables 2 and 4, respectively). Tables 5 and 6, respectively, give the relative spin-state energies of FeF_2 calculated by M06 and MR-ACPF. Both these methods predict quintet as the ground spin state, and triplet and singlet as the next two higher energy states. Previous studies with various single- and multi-reference methods[85,86,87,88] have also predicted that the ground spin state of FeF_2 is quintet ($^5\Delta$), which can be expected because F^- ligand is a weak-field ligand. In Table 5, the M06 triplet and singlet relative energies for the HOS states are underestimated compared to MR-ACPF in Table 6, which is mainly due to spin contamination. Like Fe^{2+} ion, we got rid of spin contamination from the triplet state by using the WABS method. The resulting relative energy becomes 51.2 kcal/mol, which deviates from the reference MR-ACPF value by less than one kcal/mol. Table 5 shows that the excited triplet and singlet states, which are the OOS and CS states, respectively, are pure spin states without spin contamination, and are higher in energy than the corresponding HOS states. Similar to the Fe^{2+} ion, this energy difference arises primarily due to different ways in which electrons can occupy the 3*d* orbitals of the triplet (and the singlet) state and is discussed in the next subsection.

Table 5. Relative energies (ΔE in kcal/mol)[a] with and without spin-projection and $\langle S^2 \rangle$ values of FeF_2 calculated using M06/cc-pwCV5Z-DK.

State	Type[b]	ΔE_{M06}	$\langle S^2 \rangle$
quintet	OOS	0.0	6.02
triplet	HOS	39.4,[c] 51.2[d]	2.94[c]
	OOS	59.0[e]	2.02[e]
singlet	HOS	49.4[c]	1.98[c]
	CS	88.0[e]	0.00[e]

[a] ΔE is calculated with respect to the quintet spin state.

[b] OOS = ordinary open-shell, HOS = hyper open-shell, CS = closed-shell

[c] variational solution

[d] obtained by the weighted-average broken-symmetry (WABS) spin-projection method of eq 1

[e] unstable solution

Table 6. Relative energies (ΔE in kcal/mol)[a] and effective numbers of unpaired electrons (n_U) of FeF_2 calculated using SA-CASSCF/cc-pwCV5Z-DK, MRCI/cc-pwCV5Z-DK, and MR-ACPF/cc-pwCV5Z-DK.[a]

State	Type[b]	Irrep[c]	$\Delta E_{SA\text{-}CASSCF}$	$ENUE_{CASSCF}$			$ENUE_{MRCI}$			$\Delta E_{MR\text{-}ACPF}$
				n_U	n_S	n_D	n_U	n_S	n_D	
quintet	OOS	A_g	0.0	4.00	4.00	4.00	4.01	4.00	4.04	0.0
	OOS	A_g	24.3	4.00	4.00	4.00	4.01	4.00	4.04	[d]
	OOS	B_{1g}	0.0	4.00	4.00	4.00	4.00	4.00	4.03	0.1
	OOS	B_{2g}	22.2	4.00	4.00	4.00	4.00	4.00	4.04	23.1
	OOS	B_{3g}	22.2	4.00	4.00	4.00	4.00	4.00	4.04	23.1
triplet	HOS	A_g	63.8	3.97	4.00	4.07	4.00	4.01	4.10	51.1
	HOS	B_{1g}	63.8	3.97	4.00	4.07	4.00	4.01	4.10	51.0
	HOS	B_{2g}	63.6	2.65	3.01	3.84	2.69	3.07	3.87	50.5
	HOS	B_{3g}	63.6	2.65	3.01	3.84	2.69	3.07	3.87	50.5
singlet	HOS	A_g	92.6	3.53	3.83	4.32	3.56	3.86	4.33	77.6
	HOS	B_{1g}	94.6	3.88	4.00	4.13	3.90	4.01	4.16	79.4
	HOS	B_{2g}	93.0	3.51	3.83	4.31	3.51	3.84	4.32	77.2
	HOS	B_{3g}	93.0	3.51	3.83	4.31	3.51	3.84	4.32	77.2

[a] ΔE is calculated with respect to the quintet spin state. ENUE denotes effective number of unpaired electrons.

[b] OOS = ordinary open-shell, HOS = hyper open-shell, CS = closed-shell

[c] Irrep = irreducible representation

[d] MR-ACPF can be calculated only for the first state in each irrep.

Orbital energy diagram. The electronic configurations of three spin states of FeF_2 are shown in Figure 3 using M06 orbital energies, and similarly to Figure 2, only the valence 3*d* orbitals are plotted. Figure 3 shows that the quintet state is an OOS, and each of triplet and singlet states have two ways of occupying electrons. The HOS state for both the spin states has four unpaired electrons and higher energy states (OOS for triplet and CS for singlet) have less than four unpaired electrons. As was already mentioned, these different ways of occupying electrons for the same spin state give significantly different energies.

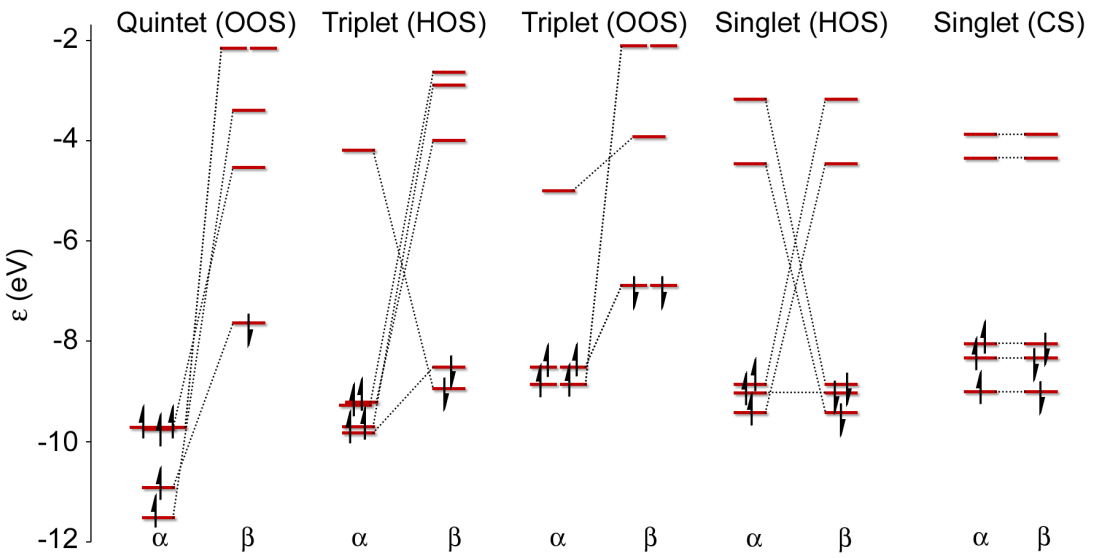

Figure 3. Orbital energy diagrams of the 3*d* orbitals of the five states (OOS quintet, HOS and OOS triplet, and HOS and CS singlet) of FeF_2 using M06/cc-pwCV5Z-DK. The dotted lines connect an orbital in the α manifold to the corresponding orbital in the β manifold. [OOS = ordinary open-shell, HOS = hyper open-shell, and CS = closed-shell]

Effective number of unpaired electrons. As we discussed for O atom and Fe^{2+} ion, because of spin contamination the number of unpaired electrons that Figure 3 gives may not be definitive, thus the effective numbers of unpaired electrons were calculated using the SA-CASSCF and MRCI wave functions. In Table 6 for all three quintet states (Δ, Π, and Σ) using both these wave function methods, the effective numbers of unpaired electrons are equal to 4.0, and they represent OOS states. Among the possible triplet states only the lowest energy states of each irrep are listed in Table 6. The effective numbers of unpaired electrons of the triplet Π (B_{2g} and B_{3g}) state are 2.69, 3.07, and 3.87 by MRCI (the CASSCF values are very similar) for n_U, n_S, and n_D approaches, respectively, which is more than the expected value of 2.00 for an OOS triplet. The effective number of unpaird electrons (3.97–4.10 for all calculations) is even higher for triplet Δ (A_g and B_{1g}) states, which lies less than 0.5 kcal/mol higher in energy than the triplet Π state. In the case of singlet states, again, only the lowest energy state of each irrep is listed in Table 6. Here the lowest energy state is a Σ (A_g) state, the first exited state is a Π (B_{2g} and B_{3g}) state, and the second excited state is a Δ (B_{1g}, its A_g component is not shown) state. For all the three singlet states, the effective numbers of unpaired electrons are larger than 3.5, *i.e.*, they are

HOS states. The HOS states of both triplet and singlet are intra-atomic as these unpaired electrons lie on the iron center and are not distributed between iron and fluorine ligands.

4. Concluding remarks

The electronic structures of O atom, Fe^{2+} ion, and FeF_2 molecule were investigated in detail using both single-reference and multi-reference methods. The DFT method used in this work is the M06 exchange–correlation functional, and the WFT methods are CASSCF, MRCI, and MR-ACPF. The high-spin state (ordinary triplet for O and ordinary quintet for Fe^{2+} and FeF_2) is the ground spin state, as predicted by all the methods. Both DFT and WFT show that the singlet of O, the lowest triplet and lowest singlet of Fe^{2+}, and the lowest triplet and lowest singlet of FeF_2 are all hyper open-shell states. The WFT method provides the most definitive characterization in terms of the number of unpaired electrons calculated from the density matrix, whereas the DFT method has the advantage of allowing one to calculate the energy lowering of the open-shell singlets as compared to closed-shell singlets. For the excited state of all three examples, the HOS state was found to be more stable than the OOS or CS state. The orbitals in the case of HOS are arranged such that it maximizes the number of unpaired electrons to achieve the number of unpaired electrons that are in the ground spin state, which leads to the total electronic energy for the HOS state being lower than the total electronic energy for the OOS or CS state. The present findings provide a new corrected perspective when compared to the conventional treatments and textbook discussions.

■ ASSOCIATED CONTENT

Supporting Information.

The Supporting Information is available free of charge on the ACS Publications website at DOI: 10.1021/

Additional spin-purification scheme and geometries. (PDF)

■ AUTHOR INFORMATION

Corresponding Authors

*E-mail: verma045@umn.edu and truhlar@umn.edu

Author Contributions

†ZV and PV contributed equally.

ORCID

Pragya Verma: 0000-0002-5722-0894
Zoltan Varga: 0000-0002-9324-798X
Donald G. Truhlar: 0000-0002-7742-7294

Notes

The authors declare no competing financial interest.

■ ACKNOWLEDGMENT

We thank Dr. Yinan Shu for help with the calculations. We also thank Alexander Boldyrev, Ernest Davidson, Francesc Illas, Yirong Mo, and Sason Shaik for feedback on the manuscript and Ernest Davidson for additional analysis that enabled us to improve the discussion. This work was funded by the U.S. Department of Energy, Office of Basic Energy Sciences, Division of Chemical Sciences, Geosciences, and Biosciences under award DE-FG02-12ER16362 as part of the Nanoporous Materials Genome Center. Partial funding from Richard D. Amelar and Arthur S. Lodge Fellowship (to PV) is acknowledged.

REFERENCES

(1) Lewis, G. N. *Chem. Rev.* **1924**, *1*, 231–248.

(2) Selwood, P. W. *Chem. Rev.* **1946**, *38*, 41–82.

(3) Dyker, G. *Angew. Chem. Int. Ed. Engl.* **1999**, *38*, 1698–1712.

(4) Alonso, J. A. *Chem. Rev.* **2000**, *100*, 637–678.

(5) Benelli, C.; Gatteschi, D. *Chem. Rev.* **2002**, *102*, 2369–2388.

(6) Shi, Z.; Zhang, C.; Tanga, C.; Jiao, N. *Chem. Soc. Rev.* **2012**, *41*, 3381–3430.

(7) Power, P. P. *Chem. Rev.* **2012**, *112*, 3482–3507.

(8) Prier, C. K.; Rankic, D. A.; MacMillan, D. W. C. *Chem. Rev.* **2013**, *113*, 5322–5363.

(9) Han, F.-S. *Chem. Soc. Rev,* **2013**, *42*, 5270–5298.

(10) Layfield, R. A. *Organometallics* **2014**, *33*, 1084–1099.

(11) Bauer, I.; Knölker, H.–J. *Chem. Rev.* **2015**, *115*, 3170–3387.

(12) Schröder, D.; Shaik, S.; Schwarz, H. *Acc. Chem. Res.* **2000***, 33*, 139−145.

(13) Harvey, J. N.; Poli, R.; Smith, K. M. *Coord. Chem. Rev.* **2003***, 238–239*, 347–361.

(14) Holland, P. L. *Acc. Chem. Res.* **2015***, 48*, 1696-1702.

(15) Davidson, E. R. *Chem. Rev.* **2000**, *100*, 351–352.

(16) Niu, S.; Hall, M. B. *Chem. Rev.* **2000**, *100*, 353–405.

(17) Furche, F.; Perdew, J. P. *J. Chem. Phys.* **2006**, *124*, 044103.

(18) Cramer, C. J.; Truhlar, D. G. *Phys. Chem. Chem. Phys.* **2009**, *11*, 10757–10816.

(19) Luo, S.; Averkiev, B.; Yang, K. R.; Xu, X.; D. G. Truhlar, D. G. *J. Chem. Theory Comput.* **2014**, *10*, 102–121.

(20) Luo, S.; Truhlar, D. G. *J. Chem. Theory Comput.* **2012**, *8*, 4112–4126.

(21) Yamaguchi, Y.; Sherrill, C. D.; Schaefer III, H. F. The $\tilde{X}\ ^3B_1$, $\tilde{a}\ ^1A_1$, $\tilde{b}\ ^1B_1$, and $\tilde{c}\ ^1A_1$ *J. Phys. Chem.* **1996**, *100*, 7911–7918.

(22) Sherrill, C. D.; Leininger, M. L.; Van Huis, T. J; Schaefer III, H. F. *J. Chem. Phys.* **1998**, *108*, 1040–1049.

(23) Bachler, V.; Olbrich, G.; Neese, F.; Wieghardt, K. *Inorg. Chem.* **2002**, *41*, 4179–4193.

(24) Fukui, H.; Kishi, R.; Minami, T.; Nagai, H.; Takahashi, H.; Kubo, T.; Kamada, K.; Ohta, K.; Champagne, B.; Botek, E.; Nakano, M. *J. Phys. Chem. A* **2008,** *112,* 8423–8429.

(25) Kamada, K.; Ohta, K.; Shimizu, A.; Kubo, T.; Kishi, R.; Takahashi, H.; Botek, E.; Champagne, B.; Nakano, M. *J. Phys. Chem. Lett.* **2010**, *1*, 937–940.

(26) Abe, M. *Chem. Rev.* **2013**, *113*, 7011–7088.

(27) Ramos-Cordoba, E.; Salvador, P. *Phys. Chem. Chem. Phys.* **2014**, *16*, 9565–9571.

(28) Borden, W. *ACS Symp. Ser.* **2015**, *1209*, 251-303.

(29) Krylov, A. I. The Quantum Chemistry of Open-Shell Species, in *Reviews in Computational Chemistry;* Parrill, A. L., Lipkowitz, K. B., Eds.; John Wiley & Sons, Inc.: Hoboken, NJ, 2017.

(30) Slipchenko, L. V.; Munsch, T. E.; Wenthold, P. G.; Krylov, A. I. *Angew. Chem. Int. Ed.* **2004**, *43*, 742–745.

(31) Cheng, L.; Wang, J.; Wangac, M.; Wu, Z. *Phys. Chem. Chem. Phys.* **2010**, *12*, 4092–4103.

(32) Shaik, S.; Chen, H.; Janardanan, D. *Nat. Chem.* **2011**, *3*, 19–27.

(33) Verma, P.; Vogiatzis, K. D.; Planas, N.; Borycz, J.; Xiao, D. J.; Long, J. R.; Gagliardi, L.; Truhlar, D. G. *J. Am. Chem. Soc.* **2015***, 137*, 5770–5781.

(34) Rajca, A. *Chem. Rev.* **1994**, *94*, 871–893.

(35) Krylov, A. I. *J. Phys. Chem. A* **2005**, *109*, 10638–10645.

(36) Ramos-Cordoba, E.; Salvador, P. *J. Chem. Theory Comput.* **2014**, *10*, 634–641.

(37) Krylov, A. I. *Acc. Chem. Res.* **2006,** *39*, 83–91.

(38) Takatsuka, K.; Fueno, T.; Yamaguchi, K. *Theor. Chim. Acta* **1978**, *48*, 175–183.

(39) Head-Gordon, M. *Chem. Phys. Lett.* **2003**, *372*, 508–511.

(40) Bochicchio, R. C.; Torre, A.; Lain, L. *Chem. Phys. Lett.* **2003**, *380*, 486–487.

(41) Head-Gordon, M. *Chem. Phys. Lett.* **2003**, *380*, 488–489.

(42) Staroverov, V. N.; Davidson, E. R. *Int. J. Quantum Chem.* **2000**, *77*, 316-323.

(43) Luzanov, A. V. Effectively Unpaired Electrons for Singlet States: From Diatomics to Graphene Nanoclusters. In Practical Aspects of Computational Chemistry IV, Leszczynski, J. Shukla, M. Eds.; Springer-Verlag: NY, 2016; Chapter 6, pp. 151–206.

(44) Vogt, N. *J. Mol. Struct.* **2001**, *570*, 189–195.

(45) Zhao, Y.; Truhlar, D. G. *J. Chem. Phys.* **2006**, *125*, 194101.

(46) Weigend, F.; Ahlrichs, R. *Phys. Chem. Chem. Phys.* **2005**, *7*, 3297–3305.

(47) Frisch, M. J.; Trucks, G. W.; Schlegel, H. B.; Scuseria, G. E.; Robb, M. A.; Cheeseman, J. R.; Scalmani, G.; Barone, V.; Mennucci, B.; Petersson, G. A.; Nakatsuji, H.; Caricato, M.; Li, X.; Hratchian, H. P.; Izmaylov, A. F.; Bloino, J.; Zheng, G.; Sonnenberg, J. L.; Hada, M.; Ehara, M.; Toyota, K.; Fukuda, R.; Hasegawa, J.; Ishida, M.; Nakajima, T.; Honda, Y.; Kitao, O.; Nakai, H.; Vreven, T.; Montgomery, J. A., Jr.; Peralta, J. E.; Ogliaro, F.; Bearpark, M.; Heyd, J. J.; Brothers, E.; Kudin, K. N.; Staroverov, V. N.; Keith, T.; Kobayashi, R.; Normand, J.; Raghavachari, K.; Rendell, A.; Burant, J. C.; Iyengar, S. S.; Tomasi, J.; Cossi, M.; Rega, N.; Millam, J. M.; Klene, M.; Knox, J. E.; Cross, J. B.; Bakken, V.; Adamo, C.; Jaramillo, J.; Gomperts, R.; Stratmann, R. E.; Yazyev, O.; Austin, A. J.; Cammi, R.; Pomelli, C.; Ochterski, J. W.; Martin, R. L.; Morokuma, K.; Zakrzewski, V. G.; Voth, G. A.; Salvador, P.; Dannenberg, J. J.; Dapprich, S.; Daniels, A. D.; Farkas, O.; Foresman, J. B.; Ortiz, J. V.; Cioslowski, J.; Fox, D. J.; *Gaussian 09*, Revision C.01; Gaussian, Inc.: Wallingford CT, 2010.

(48) Čižek, J.; Paldus, J. *J. Chem. Phys.* **1967***, 47*, 3976–3985.

(49) Seeger, R.; Pople, J. A. *J. Chem. Phys.* **1977***, 66*, 3045–3050.

(50) Bauernschmitt, R.; Ahlrichs, R. *J. Chem. Phys.* **1996***, 104*, 9047–9052.

(51) Görling, A. *Phys. Rev. A* **1993**, *47*, 2783-2799.

(52) Verma, P.; Varga, Z.; Klein, J. E. M. N.; Cramer, C. J.; Que, Jr., L.; Truhlar, D. G. *Phys. Chem. Chem. Phys.* **2017**, *19*, 13049–13069.

(53) Balabanov, N. B.; Peterson, K. A. *J. Chem. Phys.* **2005**, *123*, 064107.

(54) Peterson, K. A; Dunning, T. H., Jr. *J. Chem. Phys.* **2002**, *117*, 10548–10560.

(55) de Jong, W. A.; Harrison, R. J.; Dixon, D. A. *J. Chem. Phys.* **2001**, *114*, 48–53.

(56) Zhao, Y.; Truhlar, D. G. *Theor. Chem. Acc.* **2008**, *120*, 215–241.

(57) Douglas, M.; Kroll, N. M. *Ann. Phys. (NY)* **1974**, *82*, 89–155.

(58) Hess, B. A. *Phys. Rev. A* **1985**, *32*, 756–763.

(59) Hess, B. A. *Phys. Rev. A* **1986**, *33*, 3742–3748.

(60) Jansen, G.; Hess, B. A. *Phys. Rev. A* **1989**, *39*, 6016–6017.

(61) Yamaguchi, K.; Yoshioka, Y.; Fueno, T. *Chem. Phys. Lett.* **1977**, *46*, 360–365.

(62) Yamaguchi, K.; Yoshioka, Y.; Takatsuka, K.; Fueno, T. *Theor. Chim. Acta* **1978**, *48*, 185–206.

(63) Yamaguchi, K.; Takahara, Y.; Fueno, T.; Houk, K. N. *Theor. Chim. Acta* **1988**, *73*, 337–364.

(64) Yamanaka, S.; Kawakami, T.; Nagao, H.; Yamaguchi, K. *Chem. Phys. Lett.* **1994**, *231*, 25–33.

(65) Kitagawa, Y.; Saito, T.; Ito, M.; Shoji, M.; Koizumi, K.; Yamanaka, S.; Kawakami, T.; Okumura, M.; Yamaguchi, K. *Chem. Phys. Lett.* **2007**, *442*, 445–450.

(66) Nishino, M.; Yamanaka, S.; Yoshioka, Y.; Yamaguchi, K. *J. Phys. Chem. A* **1997**, *101*, 705–712.

(67) Noodleman, L.; Han, W. G. *J. Biol. Inorg. Chem.* **2006**, *11*, 674–694.

(68)Werner, H.-J.; Knowles, P. J.; Knizia, G.; Manby, F. R.; Schütz, M.; Celani, P.; Korona, T.; Lindh, R.; Mitrushenkov, A.; Rauhut, G.; Shamasundar, K. R.; Adler, T. B.; Amos, R. D.; Bernhardsson, A.; Berning, A.; Cooper, D. L.; Deegan, M. J. O.; Dobbyn, A. J.; Eckert, F.; Goll, E.; Hampel, C.; Hesselmann, A.; Hetzer, G.; Hrenar, T.; Jansen, G.; Köppl, C.; Liu, Y.; Lloyd, A. W.; Mata, R. A.; May, A. J.; Mcnicholas, S. J.; Meyer, W.; Mura, M. E.; Nicklass, A.; O'Neill, D. P.; Palmieri, P.; Peng, D.; Pflüger, K.; Pitzer, R.; Reiher, M.; Shiozaki, T.; Stoll, H.; Stone, A. J.; Tarroni, R.; Thorsteinsson, T.; Wang, M. *Molpro*, version 2012.1, A package of ab initio programs. See http://www.molpro.net.

(69) Werner, H.-J.; Knowles, P. J.; Knizia, G.; Manby, F. R.; Schütz, M. *WIREs Comput. Mol. Sci.* **2012**, *2*, 242–253.

(70) Roos, B. O. *Int. J. Quantum Chem., Symp.* **1980**, *14*, 175–189.

(71) Werner, H.–J.; Knowles, P. J. *J. Chem. Phys.* **1985**, *82*, 5053–5061.

(72) Knowles, P. J.; Werner, H.–J. *Chem. Phys. Lett.* **1985**, *115*, 259–267.

(73) Gdanitz, R. J.; Ahlrichs, R. *Chem. Phys. Lett.* **1988**, *143*, 413–420.

(74) Werner, H.-J.; Knowles, P. J. *Theor. Chim. Acta* **1990**, *78*, 175–187.

(75) Werner, H.-J.; Knowles, P. J. *J. Chem. Phys.* **1988**, *89*, 5803–5814.

(76) Knowles, P. J.; Werner, H.-J. *Chem. Phys. Lett.* **1988**, *145*, 514–522.

(77) Knowles, P. J.; Werner, H.-J. *Theor. Chim. Acta* **1992**, *84*, 95–103.

(78) Staroverov, V. N.; Davidson, E. R. *Chem. Phys. Lett.* **2000**, *330*, 161-168.

(79) Clark, A. E.; Davidson, E. R. *J. Chem. Phys.* **2001**, *115*, 7382-7392.

(80) Davidson, E. R.; Clark, A. E. *Mol. Phys.* **2002**, *100*, 373-383.

(81) Cañada-Vilalta, C.; O'Brien, T. A.; Brechin, E. K.; Pink, M.; Davidson, E. R.; Christou, G. *Inorg. Chem.* **2004***, 43,* 5505-5521.

(82) Kramida, A.; Ralchenko, Y.; Reader, J. and NIST ASD Team; *NIST Atomic Spectra Database* (version 5.4), [Online]. Available https://physics.nist.gov/cgi-bin/ASD/energy1.pl [accessed June 9, 2017]. National Institute of Standards and Technology: Gaithersburg, MD, 2016.

(83) https://three.jsc.nasa.gov/articles/RadChemO2Sidebar.pdf (accessed May 23, 2017).

(84) Ess, D. H.; Cook, T. C. *J. Phys. Chem. A* **2012**, *116*, 4922–4929.

(85) Wang, S. G.; Schwarz, W. H. E. *J. Chem. Phys.* **1998**, *109*, 7252–7262.

(86) Sliznev, V. V.; Vogt, N.; Vogt, J. *J. Mol. Struct.* **2006**, *780–781*, 247–259.

(87) Solomonik, V. G.; Stanton, J. F.; Boggs J. E. *J. Chem. Phys.* **2008**, *128*, 244104.

(88) Varga, Z.; Kolonits, M.; Hargittai, M. *Struct. Chem.* **2011**, *22*, 327–336.

Table-of-contents graphic: